

Powder Snow Avalanche Engineering: New Methods to Calculate Air-Blast Pressures for Hazard Mapping

Lukas Stoffel¹; Stefan Margreth²; Mark Schaer²; Marc Christen²; Yves Bühler²; Perry Bartelt²

ABSTRACT

Powder snow avalanches are a common hazard in high alpine regions. Steep tracks and cold snow temperatures facilitate the formation of the powder suspension cloud developing from the dense, fast-moving avalanche core. Considerable damage to buildings and power lines is possible even when the dense core of the avalanche stops before reaching the infrastructure. An efficient simulation tool that calculates powder pressures in three-dimensional terrain would help engineers plan mitigation measures. We present a novel two-layer powder avalanche model that couples the cloud to the flowing core, allowing the simulation of mixed flowing/powder avalanches. The model predicts endangered areas outside the reach of the dense core. We apply this model to a well-documented case study in southern Switzerland and discuss the potential for future engineering applications.

KEYWORDS

avalanche;avalanche dynamics;Modeling;Hazard Assessment.

INTRODUCTION: HAZARD MAPPING AND POWDER SNOW AVALANCHE DYNAMICS

The yellow hazard zone was introduced into Swiss snow avalanche hazard mapping procedures to account for powder avalanches with a 300 year return period and pressures smaller than 3 kPa (RL, 1984). The yellow zone is placed between the blue and white hazard zones and allows engineers to consider destructive pressures beyond the reach of the dense flowing avalanche core. For example, in the yellow zone, exposed building components must be dimensioned to withstand the wind-like blast arising from the powder cloud. Although powder avalanche pressures are small in comparison to the pressure of the dense avalanche core, they can work over the entire height of a tall structure, leading to significant overturning moments and failure. Power line cables are especially vulnerable to the air-blast which can reach significant heights above the ground. Hazard engineers use the yellow zone to signal that there is danger for persons outside buildings that might be hit by hard snow granules, woody debris or rocks that are transported by the powder cloud.

Numerical dense flow avalanche models are now in widespread application throughout the world to predict impact pressures of the flowing core, e.g. Christen (2010) and Sampl and Zwinger (2004). Flowing avalanche pressures primarily define the red and blue danger zone. If the hazard engineer, however, expects extreme powder snow avalanche activity, there are

1 WSL Institute for Snow and Avalanche Research SLF, Davos Dorf, SWITZERLAND, stoffell@slf.ch

2 WSL Institute for Snow and Avalanche Research SLF

few practical (and computationally efficient) models that can be employed to predict powder avalanche air-blast pressures.

Powder avalanche engineering/modeling is especially difficult because many questions center around the influence of terrain features. As the momentum of the powder cloud is acquired from the avalanche core, terrain features in the transition zone are of great importance. For example, steep terrain segments in the transition zone serve to accelerate the avalanche core and therefore provide sufficient forward inertia to the cloud. Steep terrain is therefore the first indicator of powder cloud formation and that the air-blast calculations are required. Terrain features that divert the direction of the avalanche core are also considered, especially when defining the lateral dispersion of the cloud (Bozhinskiy and Losev, 1998; Bühler et al., 2011). The momentum imparted to the cloud will carry it forward in the direction of the core. As the cloud is less sensitive to ground features at the avalanche base, terrain features serve to separate the core from the cloud. Significant powder avalanche pressures can therefore be generated in the transition and runout zone at the lateral edges of the avalanche track – in both the transition and runout zones (Grigoryan et al., 1982). The hazard engineer therefore must identify terrain feature that potentially cause a flow separation. This is very difficult to do without models that consider both the motion of avalanche core and powder cloud in three-dimensional terrain.

Snow climatology, avalanche volume, amount of snow entrainment and track elevation should also be considered when deciding if the powder avalanche pressures are relevant. Cold snow temperatures facilitate powder avalanche formation. Dry-cold-snow granules produce avalanche cores that fluidize and are less dense, resulting in faster flows. This allows the intake of air into the avalanche. The air becomes loaded with ice dust and is eventually blown-out of the avalanche to create the powder cloud (Bartelt et al., 2015). The temperature of the avalanche core is in large part determined by the temperature of the entrained snow (Vera Valero et al., 2015). The snowcover is, in general, colder at higher elevations. At warm temperatures, the liquid water film at the surface of snow crystals assists the bonding of stray crystals and the formation of large, heavy snow clumps (Bartelt and McARDell, 2011). Therefore, at colder temperatures it is easier to produce powder avalanches. Steep avalanche tracks with large release volumes and with potential for snow entrainment are therefore primary candidates for powder snow avalanches in cold climates and high elevations.

In this paper we present a new two-layer powder avalanche model that facilitates the calculations of air-blast pressures. A salient feature of the model is the consideration of both the avalanche core and the suspension cloud (Bartelt et al., 2015). The model is three-dimensional and accounts for snow entrainment. We apply the model to simulate the well-documented 1999 All'Acqua avalanche to demonstrate how air-blast pressures can be calculated outside the domain of the dense avalanche core.

METHODS : TWO-LAYER MIXED FLOWING/POWDER AVALANCHE DYNAMICS MODELS

To model powder snow avalanches, we apply the two-layer model of Bartelt et al. (2015) which has been implemented in the research version of the RAMMS (Christen et al., 2010) avalanche dynamics program. Two-layer models consist of an avalanche core Φ and a powder cloud Π (Figure 1). Two-layer models were first proposed by Russian scientists in the former Soviet Union (Bozhinskiy and Losev, 1998). They have also been applied to calculate powder avalanche pressures in the European alps (Naaim and Gurer, 1998; Issler 1998). The cloud Π is treated as an inertial flow arising from avalanche core Φ . The yellow zone is therefore defined by the attenuation of the powder cloud velocity after it detaches from the core. The density of the core is not constant – allowing dilute, disperse and dense flow densities. At the avalanche front, the core is dilute (“saltation layer”), allowing the intake of air Λ . This air is mixed with ice dust and blown out to create the powder cloud. For more details about the avalanche model, see Bartelt et al. (2015).

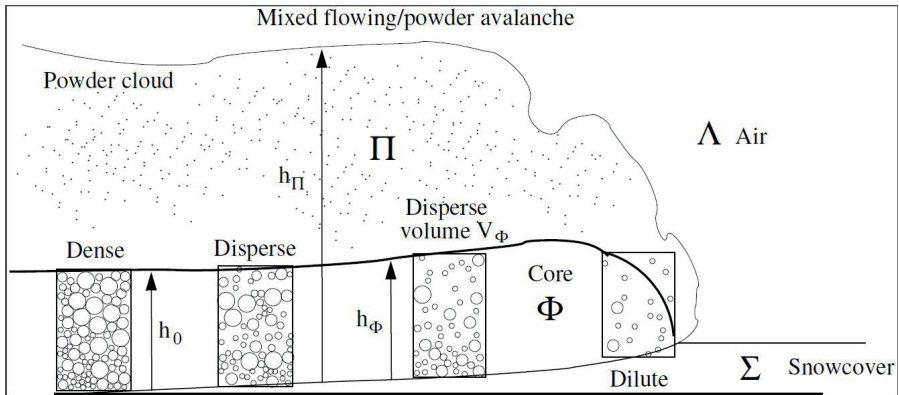


Figure 1: The structure of a mixed flowing/powder avalanche. The avalanche contains a dilute core Φ (often termed the “saltation layer”) and the powder cloud Π . The cloud can decouple from the core and move independently. Snow Σ and air Λ are entrained by the avalanche.

The model state variables for the core are,

$$\mathbf{U}_\Phi = (M_\Phi, M_\Phi u_\Phi, M_\Phi v_\Phi, Rh_\Phi, h_\Phi, M_\Phi w_\Phi, N_K)^T \quad (1)$$

and for the cloud,

$$\mathbf{U}_\Pi = (M_\Pi, M_\Pi u_\Pi, M_\Pi v_\Pi, h_\Pi)^T. \quad (2)$$

The slope parallel flow velocity of the core is given by the two-dimensional vector $\mathbf{u}_\Phi = (u_\Phi, v_\Phi)^T$, similarly for the powder cloud, $\mathbf{u}_\Pi = (u_\Pi, v_\Pi)^T$. The velocity of the avalanche core in the slope perpendicular direction is \mathbf{w}_Φ . This velocity can be considered the initial blow-out velocity of the plume structures of the powder cloud. This upward velocity should be

carefully studied to predict forces acting on powder cables suspended well-above the avalanche core. Slope-perpendicular velocities are generated when the free mechanical energy \mathbf{R} of the avalanche is deflected at the basal boundary, creating the dispersive pressure N_K (Buser and Bartelt, 2015). The dispersive pressure is associated with the inelastic scattering of snow granules and fluidization of the core and therefore the formation of so-called “saltation layers”. Core and cloud masses per unit area are denoted M_ϕ and M_Π , respectively. Flow heights measured from the basal boundary for the core and the cloud are designated h_ϕ and h_Π .

The motion of the mixed avalanche is found by solving the differential vector equations:

$$\frac{\partial \mathbf{U}_\phi}{\partial t} + \frac{\partial \Phi_x}{\partial x} + \frac{\partial \Phi_y}{\partial y} = \mathbf{G}_\phi \quad \text{and} \quad \frac{\partial \mathbf{U}_\Pi}{\partial t} + \frac{\partial \Pi_x}{\partial x} + \frac{\partial \Pi_y}{\partial y} = \mathbf{G}_\Pi \quad (3)$$

for the core and cloud layers, respectively. The flux components for the core $(\Phi_x, \Phi_y)^T$ and cloud $(\Pi_x, \Pi_y)^T$ are defined in Bartelt et al. (2015) and are not of interest here. Of greater practical interest are the components of the vectors \mathbf{G}_ϕ and \mathbf{G}_Π describing the friction and entrainment processes acting on the core ϕ and cloud Π . These are,

$$\mathbf{G}_\phi = \begin{pmatrix} M_{\Sigma \rightarrow \phi} - M_{\phi \rightarrow \Pi} \\ G_x - S_{\phi x} - M_{\phi \rightarrow \Pi} u_\phi \\ G_y - S_{\phi y} - M_{\phi \rightarrow \Pi} v_\phi \\ \alpha (\mathbf{S}_\phi \cdot \mathbf{u}_\phi) - \beta R_K \\ w_\phi \\ N_K \\ 2\gamma P - 2Nw_\phi / h_\phi \end{pmatrix} \quad \text{and} \quad \mathbf{G}_\Pi = \begin{pmatrix} M_{\phi \rightarrow \Pi} + M_{\Lambda \rightarrow \Pi} \\ M_{\phi \rightarrow \Pi} u_\phi - S_{\Pi x} \\ M_{\phi \rightarrow \Pi} v_\phi - S_{\Pi y} \\ V_{\phi \rightarrow \Pi} + V_{\Lambda \rightarrow \Pi} \end{pmatrix} \quad (4)$$

The core of the avalanche is driven by the gravitational acceleration in the slope-parallel directions $\mathbf{G} = (G_x, G_y) = (M_\phi g_x, M_\phi g_y)$. Gravitational acceleration is decomposed into three gravitational components, $\mathbf{g} = (g_x, g_y, g_z)$. The mass exchanges in the mixed flowing avalanche system are: snow entrainment into the avalanche core $M_{\Sigma \rightarrow \phi}$, volume and mass blow-out of ice-dust from the core $V_{\phi \rightarrow \Pi}$ and $M_{\phi \rightarrow \Pi}$ and direct air entrainment into the powder cloud $V_{\Lambda \rightarrow \Pi}$ (volume) and $M_{\Lambda \rightarrow \Pi}$ (mass).

Central to the model equations is the inclusion of the free mechanical energy \mathbf{R} of the avalanche core which is the sum of the energy of the random granule motions \mathbf{R}_K and configurational (density) changes \mathbf{R}_V (Buser and Bartelt, 2015). The total free mechanical energy is produced from the rate of working of the total shear $\mathbf{S}_\phi \cdot \mathbf{u}_\phi$, the model parameter α describing the production rate $0 \leq \alpha \leq 0.20$ (Buser and Bartelt, 2015). The kinetic part of the fluctuation energy \mathbf{R}_K decays according to the parameter β because of irreversible collisional/frictional interactions in the avalanche core. The parameter β is very dependent on the snow temperature.

For shearing in the core $\mathbf{S}_\Phi = (S_{\Phi_x}, S_{\Phi_y})$ we use a Voellmy-type ansatz

$$\mathbf{S}_\Phi = \frac{\mathbf{u}_\Pi}{\|\mathbf{u}_\Pi\|} \left[\mu(R_V)N + \rho_\Phi g \frac{\|\mathbf{u}_\Phi\|^2}{\xi_\Phi(R_V)} \right] \quad (5)$$

The normal pressure N includes the self-weight of the avalanche, centripetal and dispersive pressures. Both the Coulomb friction $\mu(R_V)$ and turbulent friction $\xi(R_V)$ depend on the configurational energy content of the core R_V , see (Bartelt et al., 2015).

Drag on the powder cloud $\mathbf{S}_\Pi = (S_{\Pi_x}, S_{\Pi_y})$ is given by a velocity squared type law

$$\mathbf{S}_\Pi = \frac{\mathbf{u}_\Pi}{\|\mathbf{u}_\Pi\|} \left[\rho_\Pi g \frac{\|\mathbf{u}_\Pi\|^2}{\xi_\Pi} \right] \quad (6)$$

The impact pressure of the powder cloud is given by

$$p_\Pi = C_D \left[\rho_\Pi \frac{\|\mathbf{u}_\Pi\|^2}{2} \right] \quad (7)$$

In the example calculations we consider only the impact on walls with $C_D=2$.

RESULTS: POWDER PRESSURE FIELD SIMULATION OF THE 1999 ALL'ACQUA AVALANCHE

To demonstrate how powder pressures can be deduced using two-layer avalanche dynamics models, we consider the well-documented 1999 All'Acqua avalanche (SLF, 1999; SLF, 2015). A large powder avalanche released spontaneously from the Poncione di Cassina Baggio (Bedretto Valley) on the 20th of February, 1999. The blast of the powder cloud damaged the chimney and solar panels of the Pianseccohütte (Fig. 2) as well as several cables of an electric power line (Fig. 2). Several buildings in the runout zone were slightly damaged. Furthermore up to 12 ha of 200 year old forest were destroyed on the lateral edges of the track and in the runout zone (Fig. 2).

A back analysis of this event revealed that (SLF, 1999; SLF, 2015):

- A 150 m wide release zone with average release depth of 2 m was observed on the east slope of the Poncione di Cassina Baggio. These observations were used to delineate the starting zone of the avalanche and define the release volume.
- The powder pressures at the Pianseccohütte were estimated to be 2 – 3 kPa. The core did not reach the hut.
- The powder pressure in the forest between the Pianseccohütte and the avalanche track were estimated to be 5 kPa.
- At 1900 m a.s.l. the cables of the BKW power line located 50 m above ground were not damaged by the powder cloud. Powder pressures are estimated to be less than 2 kPa.

- At 1700 m a.s.l. the cables of the ATEL powder line located 15 m above ground were cut and three masts overturned. The estimated pressures were calculated to be between 2 kPa and 5 kPa.
- Moderate forest damage at the valley bottom and at run-up counter slope indicate that powder pressures were approximately 2 kPa between 5 m and 15 m above ground.

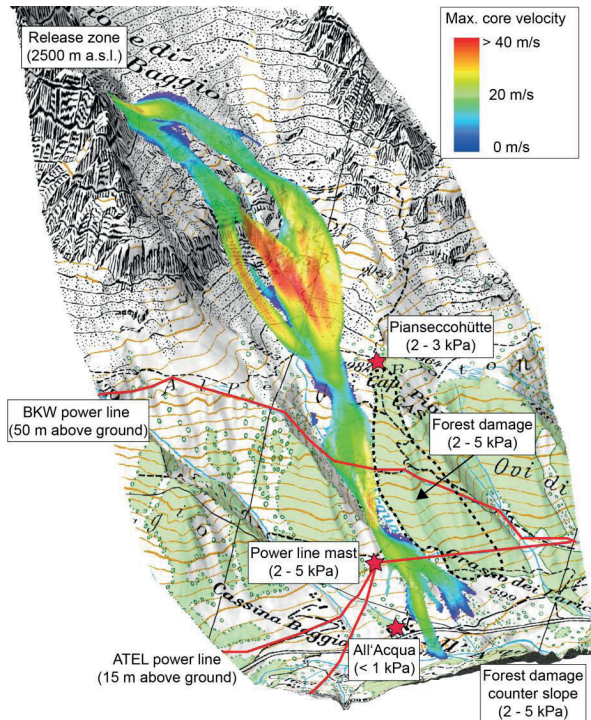


Figure 2: The All'Acqua avalanche track with the calculated maximum core velocity. The figure depicts the starting zone (2500 m), the Piansecchhütte (1985 m), the BFW power line located 50 m above ground (1900 m), the ATEL power line, located 15 m above ground (1700 m), the runout zone, the stream and counter slope and the buildings of All'Acqua (1600 m).

The simulations reveal that after release the core of the avalanche split into two distinct flow arms (Fig. 2). At 2200 m a.s.l. the avalanche descended over steep cliffs, reaching a maximum flow velocity of some 35 m/s. The two flow arms combined at 2000 m a.s.l. and managed to traverse a 300 m long flat track segment (slope inclination 10°), slowing to a velocity of 20 m/s. The avalanche core passed 120 m from the Piansecchhütte (Fig. 2).

The avalanche then reached a steeper channel section and accelerated to 35 m/s, passing under the two power lines (Fig. 2). In the runout zone the avalanche core split into two flow fingers, one finger crossed the road and reached the stream at the valley bottom, 100 m after the road (Fig. 2). The core did not travel up the counter slope. One flow arm passed only 30 m – 50 m from several buildings located in All'Acqua.

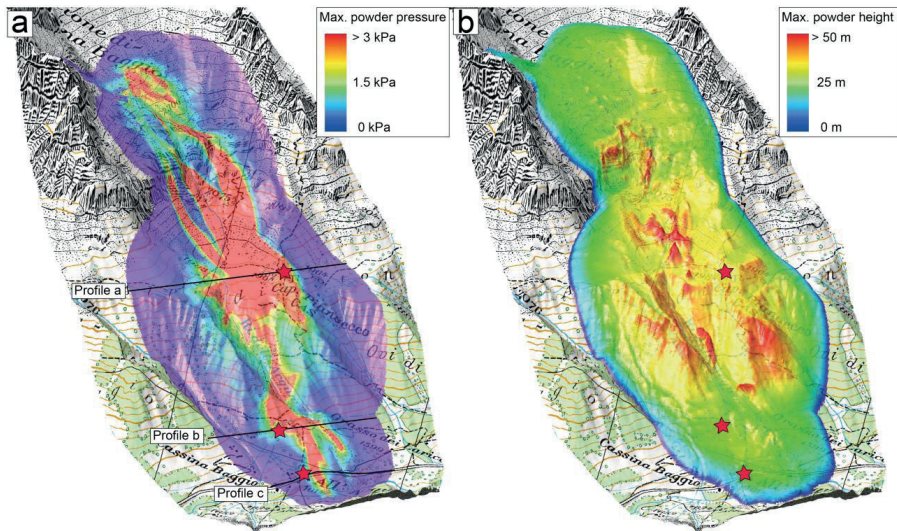


Figure 3: a) Maximum powder pressures. Location of profiles. Profile a: Piansecchöhütte. Profile b: ATEL power line. Profile c: Road, All'Acqua. b) Calculated maximum powder cloud heights and final extent of powder cloud. Model parameters: $h_0 = 1.5\text{ m}$, $\rho_0 = 250\text{ kg/m}^3$, $V_0 = 38'000\text{ m}^3$, $h_z = 0.5\text{ m}$, $\rho_z = 200\text{ kg/m}^3$, $\mu_0 = 0.55$, $\xi_0 = 2500\text{ m/s}^2$, $\alpha = 0.07$, $\beta = 0.65\text{ 1/s}$, $R_0 = 2\text{ kJ/m}^3$.

A major result in the model calculations is the difference between the simulated pressure at the Piansecchöhütte (approximately 3 kPa) and the buildings located in the runout zone at All'Acqua (less than 1 kPa). The calculated powder snow avalanche pressures at the Piansecchöhütte were larger, although the building is located 120 m from the flowing core. The calculated air-blast pressures at All'Acqua are smaller although the buildings are located only 30 m from the runout finger of the avalanche core. This result is due to terrain effects. The hut is located directly in the flow direction of the core as it descends over the cliffs. At this point the core reaches velocities up to 40 m/s. The core is later deflected but the powder cloud travels towards the Piansecchöhütte. At the valley bottom in All'Acqua, the houses are not in the primary direction of the core. A comparison of the pressures profiles a and c (defined in Fig. 3), reveals a large difference in the lateral attenuation of powder pressure: at the Piansecchöhütte the air-blast pressure attenuates over a distance of approximately 160 m (Fig. 4a); at All'Acqua the pressure attenuates over a distance of 50 m (Fig. 4c).

Large air-blast pressures (between 6 kPa and 10 kPa) were predicted at the location where the avalanche crossed the ATEL power line (Fig. 4d). Maximum flow densities of the powder cloud varied between 4.5 kg/m³ and 5.0 kg/m³. In two-layer models these pressures represent the mean pressure exerted by the powder cloud. When the avalanche is a pure powder avalanche this region extends from the ground to the top of the cloud. The calculated powder cloud heights at the front of the avalanche (where the pressures are highest) are between 15 m and 20 m (Fig. 4d). The heights eventually increase to heights over 50 m

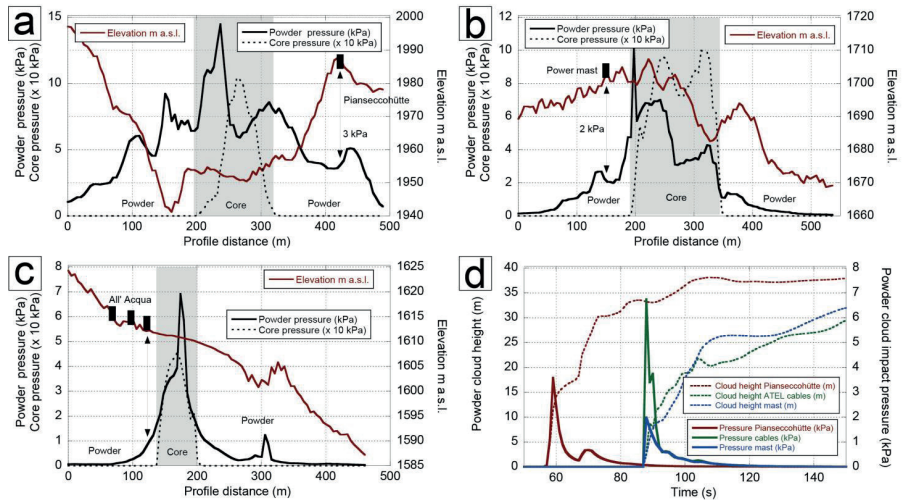


Figure 4: a) Lateral attenuation of powder pressure at the profile a (Fig. 3a), Pianseccohütte. b) Attenuation of powder pressures at the ATEL power line, profile b (Fig. 3a). c) Powder profile at the road, profile c (Fig. 3a). d) Calculated powder cloud height and pressure at Pianseccohütte, ATEL power line and ATEL power line mast.

(Fig. 3b). Therefore, the model predicts the ATEL cables are clearly vulnerable, although the two-layer model does not predict the attenuation of pressure with increasing height. At present we assume uniform depth profiles for velocity and density.

Calculated pressures at the power mast are 2 kPa; calculated heights are 10 m, quickly rising to 25 m (Fig. 4d). These, coupled with the forces on the cables, would be sufficient to overturn the mast. At the upper power line (BKW) the calculated heights at the front of the avalanche are between 20 m and 30 m, lower than the 50 m suspension height of the cables (Fig. 3b).

Finally, we note that the calculated pressures in the forested regions (Fig. 2) are enough to blow-down trees (Feistl et al., 2015). The regions of highest pressures (over 3 kPa) are located in the forest regions near the Pianseccohütte and between the two power lines (Fig. 3b). Calculated pressures on the counter slope (between 1 kPa and 2 kPa) are enough to cause isolated tree blow-downs (Fig. 3b).

CONCLUSIONS

In this paper we applied the research version of RAMMS, a two-layer numerical avalanche dynamics model, to simulate the spatial distribution of powder avalanche pressure in three-dimensional terrain. We are particularly interested in the pressures beyond the reach of the flowing avalanche core, as these pressures are used (1) to delineate yellow hazard zones, (2) identify regions of powder avalanche destruction (forests, buildings) and (3)

calculate powder pressures on objects such as power lines, located some vertical distance above the flowing avalanche. We treat the powder cloud as an inertial flow: air is taken in by the avalanche core, loaded with ice-dust and blown-out with the speed of the flowing core. Once formed the powder cloud moves independently of the avalanche core. The primary flow direction and speed of the powder cloud is defined by the velocity of the core. The attenuation of the powder cloud speed (drag, Eq. 6) defines the magnitude of the powder cloud pressure outside the domain of the flowing core.

Our simulation of the All'Acqua avalanche event indicate that because two-layer models simulate the movement of the core and cloud they allow the inclusion of important terrain effects which determine the area endangered by powder pressures, especially at the lateral edges of the avalanche. One-dimensional models are not able to reproduce these features. The model calculates the powder cloud height, speed and mean pressure, but does not predict the attenuation of pressure with height. For this purpose, we do not believe that three-dimensional calculations are necessary, as these are computationally expensive; however, an engineering method is still out-standing. For this purpose, it will be necessary to redesign the experimental test sites to obtain measurements that validate an analytical pressure function.

REFERENCES

- Bartelt P., Buser O., Vera Valero C., Bühler Y. (2015) Configurational energy and the formation of mixed flowing/powder snow and ice avalanches, *Annals of Glaciology*, 71.
- Bartelt P. and McArdell B. (2009). Granulometric investigations of snow avalanches. *J. Glaciol.*, 55(193), 829–833 (doi: 10.3189/002214309790152384).
- Bozhinskiy AN and Losev KS. (1998). The fundamentals of avalanche science [transl. CE Bartelt]. Eidg. Inst. Schnee- und Lawinenforsch. Mitt. 55.
- Bühler Y., Christen M., Kowalski J., Bartelt P. (2011) Sensitivity of snow avalanche simulations to digital elevation model quality and resolution. *Ann. Glaciol.* 52, 58, 72-80.
- Buser O. and Bartelt P. (2015). An energy-based method to calculate streamwise density variations in snow avalanches, *Journal of Glaciology*, 61(227), doi: 10.3189/2015JoG14J054.
- Christen M., Kowalski J., Bartelt P. (2010). RAMMS: Numerical simulation of dense snow avalanches in three-dimensional terrain, *Cold Regions Science and Technology*, doi:10.1016/j.coldregions.2010.04.005.
- Dreier L., Bühler Y., Ginzler C., Bartelt P. (2015). Comparison of simulated powder snow velocities, volumes and flow widths with photogrammetric measurements, *Annals of Glaciology*, in press.
- Feistl, T., Bebi, P., Christen, M., Margreth, S., Diefenbach, L., and Bartelt, P. (2015). Forest damage and snow avalanche flow regime, *Nat. Hazards Earth Syst. Sci.*, 15, 1275-1288, doi:10.5194/nhess-15-1275-2015.
- Grigoryan S., Urubayev N. and Nekrasov I. (1982). Experimental'noye issledovaniye lav innoy vozdushnoy volny [Experimental investigation of an avalanche air blast]. *Mater. Glyatsiol. Issled.*,

44, 87–93 [in Russian].

- Issler, D. (1998) Modelling of snow entrainment and deposition in powder snow avalanches, *Annals of Glaciology*, 26, 253 – 258.
- Naaim, M. Gurer, I. (1998). Two-phase numerical model of powder avalanche: theory and application, *Natural Hazards*, 117, 129-145.
- RL (1984). Richtlinien zur Berücksichtigung der Lawinengefahr bei raumwirksamen Tätigkeiten. Bundesamt für Forstwesen, Eidg. Institut für Schnee- und Lawinenforschung.
- Sampl, P., Zwinger, T., (2004). Avalanche simulation with SAMOS. *Annals of Glaciology*, 38, 393-398.
- SLF (1999). Lawinengefährdung der ATEL 380/220kV Leitung Airolo–Ponte(I) im Bereich All’Acqua Bedretto (TI), SLF Gutachten G 99.13.
- SLF (2015). Lawineneinwirkungen auf die Piansecchöhütte CAS/SAC, Bedretto (TI), SLF Gutachten G 2015.06.
- Vera Valero C., Wikstroem Jones K., Bühler Y., Batelt, P. (2015). Release temperature, snow-cover entrainment and the thermal flow regime of snow avalanches, *Journal of Glaciology*, Vol. 61, No. 225, doi: 10.3189/2015JoG14J117.